CERN-TH/95-103
SMU HEP 95-02

CHARM PRODUCTION IN DEEP-INELASTIC $e\gamma$ SCATTERING TO NEXT-TO-LEADING ORDER IN QCD [1]

Eric Laenen
CERN TH-Division
1211-CH, Geneve 23, Switzerland

and

Stephan Riemersma
Department of Physics, Fondren Science Building
Southern Methodist University, Dallas, TX 75275, U.S.A

Abstract

We discuss the calculation of F_2^γ(charm) to next-to-leading order (NLO) in QCD, including contributions from both hadronlike and point-like photons. We show that the former dominates strongly below $x \simeq 0.01$, and the latter above this value. This fact makes F_2^γ(charm) for $x \geq 0.01$ calculable, whereas for $x \leq 0.01$ it serves to constrain the small-x gluon density in the photon. Both ranges in x are accessible at LEP2. Theoretical uncertainties are well under control. We present rates for single-tag events for the process for $e^+e^- \to e^+e^-cX$ for LEP2. Although these event rates are small, we believe a measurement of F_2^γ(charm) is feasible.

CERN-TH/95-103
SMU HEP 95-02
May 1995

[1] Talk presented by E. Laenen at Photon'95, Sheffield, UK, April 8-13, 1995.

Open heavy quark production in two-photon collisions at e^+e^- colliders has been difficult to observe in experiments. This is mostly due to the typically small cross section coupled with low charm tagging efficiencies. At LEP1 an additional difficulty is represented by the Z^0 background, from which a two-photon sample is hard to isolate. Experimentally one has studied the reaction $e^+e^- \to e^+e^- D^{*\pm} X$ with neither outgoing lepton tagged ("no-tag"), because it proceeds predominantly via the fusion of two equivalent photons to produce open charm ($\gamma\gamma \to c\bar{c}$). Measurements of the $D^{*\pm}$ cross section in no-tag e^+e^- collisions have been performed by JADE, TASSO, TPC/2γ, TOPAZ, VENUS, ALEPH and AMY. [1].

The equivalent measurement for the case in which one of the outgoing leptons is tagged ("single-tag") has not been performed. The demand for the extra tag suppresses the rate too much for present experiments to measure.

The theory is in better shape. The cross section for $\gamma\gamma \to c\bar{c}$ has been calculated to next-to-leading (NLO) order in QCD in [2], and found to agree quite well with experimental results. Here we focus on the single-tag case. We begin in general by considering the reaction

$$e^-(p_e) + e^+ \to e^-(p'_e) + e^+ + X\,, \tag{1}$$

where X denotes any hadronic state allowed by quantum-number conservation laws. When the outgoing electron is tagged then this reaction is dominated by the subprocess

$$\gamma^*(q) + \gamma(k) \to X\,, \tag{2}$$

where one of the photons is highly virtual and the other one is almost on-mass-shell. The case where the positron is tagged is completely equivalent. This process is described by the cross section

$$\begin{aligned} \frac{d^2\sigma}{dx dQ^2} &= \int dz\, z\, f_\gamma^e(z, \frac{S}{m_e^2})\, \frac{2\pi\alpha^2}{x\, Q^4} \\ &\quad \times \left[\{1 + (1-y)^2\} F_2^\gamma(x, Q^2) - y^2 F_L^\gamma(x, Q^2)\right]\,, \end{aligned} \tag{3}$$

where the $F_k^\gamma(x, Q^2)$ $(k = 2, L)$ denote the deep-inelastic photon structure functions and $\alpha = e^2/4\pi$ is the fine structure constant. The Bjorken scaling variables x and y are defined by

$$x = \frac{Q^2}{2k\cdot q}\,, \qquad y = \frac{k\cdot q}{k\cdot p_e}\,, \qquad q = p_e - p'_e\,, \tag{4}$$

where p_e, p'_e are defined in (1). The off-mass-shell photon and the on-mass-shell photon have four-momenta q and k respectively with $q^2 = -Q^2 < 0$ and $k^2 \approx 0$. Because the photon with momentum k is almost on-mass-shell, eq. (3) is written in the Weizsäcker-Williams approximation: the function $f^e_\gamma(z, S/m_e^2)$ represents the probability of finding a photon $\gamma(k)$ in the positron, with longitudinal momentum fraction z, and is given in first approximation by

$$f^e_\gamma(z, \frac{S}{m_e^2}) = \frac{\alpha}{2\pi} \frac{1+(1-z)^2}{z} \ln \frac{(1-z)(zS-4m^2)}{z^2 m_e^2}\,, \tag{5}$$

provided a heavy quark with mass m is produced (for light quarks $m = 0$). Here S is the c.m. energy squared of the electron-positron system.

In (3) both structure functions can be represented as

$$F^\gamma_k(x, Q^2) = \sum_{i=q,\bar{q},g} f^\gamma_i \otimes C_{k,i}(\frac{Q^2}{\mu_f^2}) + C_{k,\gamma}(\frac{Q^2}{\mu_f^2}). \tag{6}$$

The f^γ_i are photonic parton densities and the $C_{k,i}\,(i = q, \bar{q}, g, \gamma)$ are Wilson coefficient functions. For the results presented here we used for the f^γ_i the GRV leading-order (LO) set for LO calculations, and the GRV higher-order (HO) set for NLO ones [3], in the $\overline{\rm MS}$ scheme. In [4] F^γ_2 and F^γ_L were calculated to NLO in QCD by computing all $O(\alpha_s)$ corrections to the coefficient functions $C_{k,i}$. For F^γ_L this represented the first NLO analysis, while for F^γ_2 the new corrections consisted of those due to the inclusion of heavy quarks. We will now focus on these heavy quark contributions to F^γ_2 for the case of charm, and highlight some of the very interesting features they possess.

Note that in (6) both terms on the right hand side depend on the mass factorization scale μ_f, which, although it may be judiciously chosen, is in principle arbitrary. If one now demands the presence of a charm quark in the final state, the μ_f dependence of the second term is not present through NLO. Splitting F^γ_2 then according to (6) as

$$F^\gamma_2(\text{charm}) = F^{\gamma,HAD}_2(x, \frac{Q^2}{\mu_f^2}, \frac{m^2}{\mu_f^2}) + F^{\gamma,PL}_2(x, \frac{Q^2}{m^2}) \tag{7}$$

this means that $F^{\gamma,PL}_2$ is completely calculable, whereas $F^{\gamma,HAD}_2$ is, analo-

gously to the proton case, mainly sensitive to the photonic gluon density.

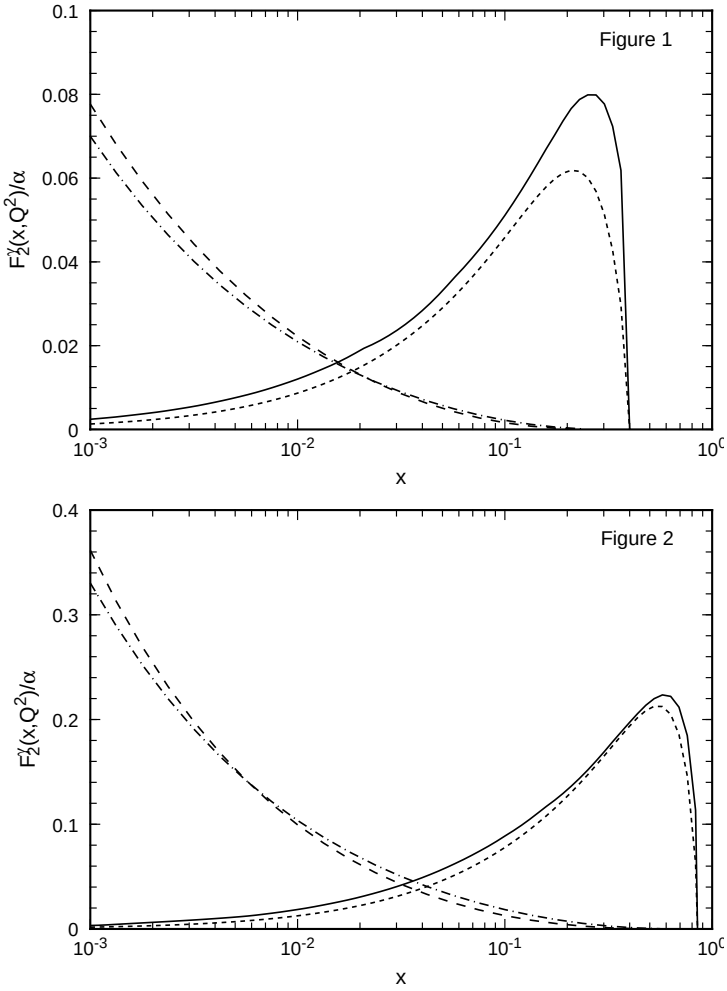

Figure 1: Hadronic and pointlike contributions to $F_2^\gamma(\text{charm})/\alpha$ at $Q^2 = 5.9\,(\text{GeV}/c)^2$. The short-dashed line denotes the LO pointlike, and the solid line the NLO pointlike component. The long-dashed line denotes the LO hadronlike, and the dot-dashed the NLO hadronlike component. Figure 2: same as in Figure 1, now at $Q^2 = 51\,(\text{GeV}/c)^2$. For both figures we used a one-loop running α_s with $\Lambda = 232\,\text{MeV}$ at LO and a two-loop running α_s with $\Lambda = 248\,\text{MeV}$ at NLO, both for three active flavors. We used a charm mass of $1.5\,\text{GeV}$.

The only uncertainties in $F_2^{\gamma,PL}(x,Q^2)$ are due to α_s and the charm mass.

At a value of $Q^2 \approx 6\,(\mathrm{GeV}/c)^2$ the uncertainty due to the latter is about 20%, and about 10% for $Q^2 \approx 50\,(\mathrm{GeV}/c)^2$, if the charm mass is varied between 1.3 and 1.8 GeV. The largest uncertainty in $F_2^{\gamma,HAD}$ is due to the small-x photonic gluon density f_g^γ, hence a measurement of $F_2^{\gamma,HAD}$ could be used to constrain f_g^γ.

Figs. 1 and 2 show $F_2^{\gamma,PL}$ and $F_2^{\gamma,HAD}$ versus x at both LO and NLO, for $Q^2 = 5.9\,(\mathrm{GeV}/c)^2$ and $Q^2 = 51\,(\mathrm{GeV}/c)^2$ respectively. Note that the $O(\alpha_s)$ corrections to $F_2^{\gamma,PL}$ are fairly small. We may thus assume that even higher order contributions are negligible, and that thus this component is calculated with some precision.

The most remarkable feature in these figures is clearly the clean separation in x of both components. As a result on may confront a precise calculation and constrain the small-x photonic gluon density in one experiment.

As mentioned earlier, such an experimental study is very difficult in practice, due to the inherently low event rate and the difficulty of efficient charm tagging. In order to judge the feasibility of such a study we have integrated (3) for various x, Q^2 bins, and obtained estimates for the number of charm quarks per bin produced at LEP2.

As an aside, in order to perform the integrals over x and Q^2, we used fitted versions of the coefficient functions $C_{k,i}$ in (6), as the actual expressions in [4] are too long for fast evaluation. By adapting the fitted coefficient functions of electroproduction of heavy quarks on a proton target [5] to our case we were able to speed up the code by as much as a factor of twenty.

For the Weizsäcker-Williams density of equivalent photons in the electron we used here the improved version of [6], which allows for an anti-tagging angle. Furthermore, in order to test the stability of the results we put the renormalization scale equal to the mass factorization scale μ_f and varied the latter from $Q/2$ to $2Q$.

The results are shown in Table 1. We have shown here the total number of events in the top half of the table, and its pointlike component in the bottom half. The hadronlike component per bin is obtained by simply taking the difference. We see that even with a charm tagging efficiency of, say, 2% on average a few tens of events per bin should be observable for larger x values. The numbers in Table 1 increase by about 40% if one uses the naíve Weizsäcker-Williams density of (5). Note that they change relatively little under variations in the factorization scale μ_f.

Given the small event rates and the interesting physics these events provide a handle to, it is clearly important to obtain the highest possible charm tagging efficiency at LEP2. The results of various methods of charm tagging have been presented at this conference [7] and there are prospects to achieve a satisfactory efficiency at LEP2.

Summarizing, we have shown the clear separation in x of the contributions to F_2^γ(charm) due to pointlike and hadronlike photons. The pointlike component is calculable in perturbative QCD, while the hadronlike component constrains the small-x gluon density in the photon.. An estimate of event rates suggests that a measurement of F_2^γ(charm), although difficult, may be feasible at LEP2, and is certainly worthwhile.

References

[1] W. Bartel et al., (JADE), *Phys.Lett.* **B184** (1987) 288; M. Alston-Garnjost et al.(TPC/2γ), *Phys.Lett.* **B252** (1990) 499; W. Braunschweig et al. (TASSO), *Z. Phys.* **C47** (1990) 499; R. Enomoto et al. (TOPAZ), *Phys.Rev.* **D50** (1994) 1879; *Phys.Lett.* **B328** (1994) 535; S. Uehara et al.(VENUS), *Z. Phys.* **C63** (1994) 213; D. Buskulic et al. (ALEPH), CERN preprint CERN-PPE-95-40. T. Nozaki, for the AMY collaboration, these proceedings.

[2] M. Drees, M. Krämer, J. Zunft and P. Zerwas, *Phys.Lett.* **B306** (1993) 371; M. Krämer, these proceedings.

[3] M. Glück, E. Reya and A. Vogt, *Phys.Rev.* **D46** (1992) 1973.

[4] E. Laenen, S. Riemersma, J. Smith and W.L. van Neerven, *Phys.Rev.* **D49** (1994) 5753.

[5] S. Riemersma, J. Smith and W.L. van Neerven, *Phys.Lett.* **B347** (1995) 143.

[6] S. Frixione, M. Mangano, P. Nason and G. Ridolfi, *Phys.Lett.* **B319** (1993) 339.

[7] T. Nozaki, these proceedings.
M. Iwasaki, these proceedings.
F. Foster, these proceedings.

Table 1. Total number of events for single-tag charm production at LEP2 ($500/pb$ integrated luminosity), based on NLO QCD, determined from eq. (1). We used the Weizsäcker-Williams density of Frixione et al. [6] with an anti-tagging angle $\theta_c = 20\,\mathrm{mrad}$, and the GRV HO set of photonic parton densities, in the $\overline{\mathrm{MS}}$ scheme [3].

Q^2 (GeV^2)	Q^2 range	x range	Events		
			$\mu_f = Q/2$	$\mu_f = Q$	$\mu_f = 2Q$
		Total			
6.6	3.2 - 10	$1.0 - 3.2 \cdot 10^{-4}$	47	45	44
		$3.2 - 10.0 \cdot 10^{-4}$	294	273	264
		$1.0 - 3.2 \cdot 10^{-3}$	571	517	494
		$3.2 - 10.0 \cdot 10^{-3}$	783	699	659
		$1.0 - 3.2 \cdot 10^{-2}$	1104	1002	949
		$3.2 - 10.0 \cdot 10^{-2}$	2091	1969	1904
		$1.0 - 3.2 \cdot 10^{-1}$	4403	4057	3873
		$3.2 - 10.0 \cdot 10^{-1}$	832	718	656
20.8	10 - 32	$3.2 - 10.0 \cdot 10^{-4}$	24	24	24
		$1.0 - 3.2 \cdot 10^{-3}$	144	138	136
		$3.2 - 10.0 \cdot 10^{-3}$	274	260	253
		$1.0 - 3.2 \cdot 10^{-2}$	409	384	371
		$3.2 - 10.0 \cdot 10^{-2}$	713	683	666
		$1.0 - 3.2 \cdot 10^{-1}$	1611	1575	1553
		$3.2 - 10.0 \cdot 10^{-1}$	1604	1519	1464
		Pointlike			
6.6	3.2 - 10	$3.2 - 10.0 \cdot 10^{-4}$	8.3	7.1	6.4
		$1.0 - 3.2 \cdot 10^{-3}$	50	43	40
		$3.2 - 10.0 \cdot 10^{-3}$	202	182	171
		$1.0 - 3.2 \cdot 10^{-2}$	644	602	579
		$3.2 - 10.0 \cdot 10^{-2}$	1846	1770	1728
		$1.0 - 3.2 \cdot 10^{-1}$	4351	4023	3846
		$3.2 - 10.0 \cdot 10^{-1}$	832	718	656
20.8	10 - 32	$1.0 - 3.2 \cdot 10^{-3}$	7.0	6.3	5.9
		$3.2 - 10.0 \cdot 10^{-3}$	42	39	37
		$1.0 - 3.2 \cdot 10^{-2}$	173	163	156
		$3.2 - 10.0 \cdot 10^{-2}$	554	537	526
		$1.0 - 3.2 \cdot 10^{-1}$	1557	1528	1509
		$3.2 - 10.0 \cdot 10^{-1}$	1602	1518	1463